# Impact of extreme wildfires from the Brazilian Forests and sugarcane burning on the air quality of the biggest megacity on South America

Carlos E. Souto-Oliveira [a,*], Márcia T.A. Marques [a], Thiago Nogueira [a,d], Fabio J.S. Lopes [b], José A.G. Medeiros [b], Ilca M.M.A. Medeiros [b,c], Gregori A. Moreira [b], Pedro Leite da Silva Dias [a], Eduardo Landulfo [b], Maria de F. Andrade [a]

[a] Institute of Astronomy, Geophysics and Atmospheric Science, University of São Paulo, Butantã, São Paulo, SP 05508-090, Brazil
[b] Nuclear and Energy Research Institute, IPEN-CNEN, Centre for Laser and Applications (CLA), São Paulo 05508-970, Brazil
[c] City University of São Paulo (UNICID), R. Cesário Galeno, 448 - Tatuapé, São Paulo, SP 03071-000, Brazil
[d] Departamento de Saúde Ambiental, Faculdade de Saúde Pública, Universidade de São Paulo, 01246-904, São Paulo, Brazil

## HIGHLIGHTS

- Risks of forest wildfire and harvest burnings to air quality and public health on megacities
- Assessment of external pollution sources to atmospheric pollution on urban areas
- Comprehensive scenario of long-range transport of smoke plumes and intrusion on urban atmosphere

## GRAPHICAL ABSTRACT
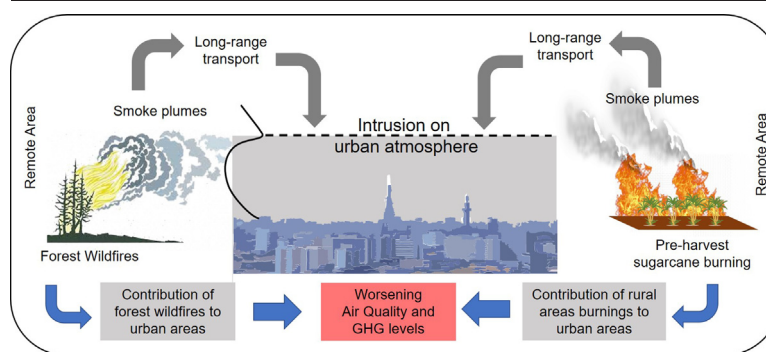


## ARTICLE INFO

## ABSTRACT

Recently, extreme wildfires have damaged important ecosystems worldwide and have affected urban areas miles away due to long-range transport of smoke plumes. We performed a comprehensive analysis to clarify how smoke plumes from Pantanal and Amazon forests wildfires and sugarcane harvest burning also from interior of the state of São Paulo (ISSP) were transported and injected into the atmosphere of the Metropolitan Area of São Paulo (MASP), where they worsened air quality and increased greenhouse gas (GHG) levels. To classify event days, multiple biomass burning fingerprints as carbon isotopes, Lidar ratio and specific compounds ratios were combined with back trajectories modeling. During smoke plume event days in the MASP fine particulate matter concentrations exceeded the WHO standard ($>25$ µg m$^{-3}$), at 99 % of the air quality monitoring stations, and peak $CO_2$ excess were 100 % to 1178 % higher than non-event days. We demonstrated how external pollution events such as wildfires pose an additional challenge for cities, regarding public health threats associated to air quality, and reinforces the importance of GHG monitoring networks to track local and remote GHG emissions and sources in urban areas.

## 1. Introduction

In comparison with historical data, temperatures worldwide were abnormally warm during 2020; the frequency and duration of heat waves also increased, as did the abundance and intensity of forest fires (NASA, 2020; WWF, 2020; Perkins-Kirkpatrick and Lewis, 2020). In recent years, wildfire activity has been more intense in various ecosystems, with environmental, health, and economic impacts, in many countries (Balch et al., 2017). The impacts of wildfires are felt not only by the communities in proximity to the fire zone but also by cities miles away, because of long-range transport of smoke plumes (Rogers et al., 2020; Reddington et al.,

2015). Human-caused wildfires and anthropogenic climate change combine to exacerbate wildfires significantly, other than non-anthropogenic contributions (Balch et al., 2017; Jolly et al., 2015; Jones et al., 2020). In this context, investigation about intrusion of smoke plumes into the atmosphere of large urban areas is imperative to assess the real impact of wildfires to millions of people.

Extensive, recurrent severe wildfires in the Amazon rainforest (Escobar, 2019; IPAM, 2020; Satar et al., 2016) have received considerable international attention for many years. However, the unprecedented wildfires in the Pantanal wetlands of Brazil in 2020 caused alarm because of their magnitude and the variety of wildlife affected (Mega, 2020; NASA, 2020). The Pantanal, which is the largest remaining wetland area of natural vegetation in the world, has been declared to be a World Heritage Site by the United Nations Educational, Scientific, and Cultural Organization, which has also designated it a Biosphere Reserve (Libonati et al., 2020). The Pantanal encompasses 179,300 km$^2$ in the center of the Upper Paraguay River Basin, 78 % of which is in Brazil (Tomas et al., 2019). The seasonal flood pulse, with a well-defined rainy season (summer), supports nutrient cycling, primary productivity, and significant biodiversity, which results in the storage of large amounts of carbon (Ivory et al., 2019; Pinto et al., 2020). The lack of efficient conservation and the failure to implement climate change mitigation strategies in the area, together with the effects of extreme meteorological events, comprises in risks to climate and the Pantanal and other Brazilian biomes (Marengo et al., 2021; Tomas et al., 2019). In 2020, roughly one third of the Pantanal burned, the wildfires destroying approximately 4 million hectares of vegetation and displacing the fauna (Libonati et al., 2020). In addition to the local effects of those unprecedented wildfires, smoke plumes, most associated with the Pantanal wildfires, and potentially combined with Amazonian wildfires, were observed during the month of September 2020 in the Metropolitan Area of São Paulo (MASP), 1000 km away.

Another important source of smoke plumes to MASP is related to preharvesting burning of sugarcane, that is a current activity used in sugarcane production in the interior of the state of São Paulo (ISSP) (Gonino et al., 2019). Current policies to eliminate fire practices in order to avoid negative effects of smoke plumes has contributed to decrease fires events, however this activity remain as an external pollutant source to MASP, placed hundreds of kilometers away (Pivello et al., 2021). Therefore, forest wildfires and sugarcane burning pose a threat to MASP air quality when combined with local sources. However, the impact of those remote sources, such as forest wildfires and sugarcane burning, was few exploited. Real impacts of external smoke plume events on air pollution in the MASP, which is the fourth largest urban agglomeration in the world (UN, 2018), with >21 million inhabitants, should be further investigated in order to understand risks to the vulnerability of this urban area and public health. According to IPCC report (IPCC, 2018), the control of climate pollutants is important for improving air quality and controlling climate change.

Here, we assess the important roles of recent Brazilian forest wildfires mainly from Amazonian and Pantanal, and sugarcane burning regarding in worsening air quality and improving greenhouse gas (GHG) levels in the largest megacity in South America. Smoke plumes arriving in the MASP were detected by satellite- and ground-based GHG and air quality measurement networks. The plume detection results were based on multiple approaches related to the fingerprints of biomass burning, such as the Raman extinction-to-backscatter ratio (LiDAR ratio), carbon isotope ratio of CO$_2$ ($\delta^{13}$C-CO$_2$), PM$_{2.5}$–CO ratio, CO/CO$_2$ ratio, CH$_4$/CO$_2$ ratio, as well as the identification of episodes of higher CO$_2$, CO, and CH$_4$ concentrations. We also performed a comprehensive analysis to understand the meteorological conditions favorable to the intrusion and accumulation of smoke plumes into the atmospheric boundary layer (ABL).

## 2. Materials and methods

### 2.1. Metropolitan area of São Paulo (MASP)

The MASP encompasses an area of 7946 km$^2$ within the state of São Paulo, located in the southeastern region of Brazil (Fig. 1a), and is the

largest urban agglomeration in South America, with >21 million inhabitants and a fleet of approximately 8 million vehicles.

### 2.2. GHG surface measurement network (METROCLIMA)

The São Paulo GHG monitoring network, established in March 2020 by a consortium of research institutes (www.metroclima.iag.usp.br), comprises three continuously operating monitoring stations, all located within the MASP (Fig. 1a): a vegetated site in a protected area in the extreme western part of the MASP (Pico do Jaraguá, PDJ); a partially vegetated, suburban site in the central-west part of the MASP, on the campus of the University of São Paulo (IAG) and an urban site in the eastern, with intense traffic in the surrounding area (UND). The monitoring stations are equipped with cavity ring-down spectroscopy instruments (Picarro) which measure CO$_2$, CH$_4$, and CO concentrations, as well as $\delta^{13}$C-CO$_2$ values, in real time.

### 2.3. CO$_2$ source apportionment

The Keeling plots were created by the distribution of the hourly average $\delta^{13}$C-CO$_2$ values versus those of 1/CO$_2$. Isotopic signatures associated with the main sources (Fig. 2b) were estimated by calculating the intercepts of the daily linear regressions. The CO$_2$ source apportionment estimation was based on the system with three end-members, such as fossil fuel (FF, $\delta^{13}$C-CO$_2$ = −30 ‰, CO/CO$_2$ = 0.5 ppm, Semmens et al., 2014; Schumacher et al., 2011), forest wildfire + wood burning (C3, $\delta^{13}$C-CO$_2$ = −25 ‰, CO/CO2 = 6 ppm, 49) and ethanol + sugarcane burning (C4, $\delta^{13}$C-CO$_2$ = −12 ‰, CO/CO$_2$ = 0.5 ppm, Neves et al., 2015), and two variables ($\delta^{13}$C-CO$_2$ and CO/CO$_2$). The mix model was solved using EPA IsoSource software, version 1.3.1.

### 2.4. Air quality data

The air quality monitoring network in MASP is operated by the São Paulo State Environmental Protection Agency (CETESB, Companhia Ambiental; cetesb.sp.gov.br) and consisted of 26 monitoring stations, which have the differences among altitude, vehicular traffic intensity, vegetation, and pollution sources. In this study, air quality data of 15 stations distributed in MASP were used (Fig. 1a). The CETESB takes charge of with measuring the concentrations of pollutants, validating emission inventories, and making databases available. To ensure the representativeness of the CO and PM$_{2.5}$ daily averages, we considered only days for which >50 % of the hourly data were available.

### 2.5. Remote sensing monitoring

The LiDAR system at the University of São Paulo (USP LiDAR station) is a multi-wavelength Raman LiDAR installed at the Brazilian Nuclear and Energy Research Institute (23°33′S, 46°38′W, at an elevation of 760 m a.s.l.). It is a coaxial ground-based system and operates with a pulsed Nd:YAG laser, at 1064, 532, and 355 nm, with laser energy per pulse of approximately 600, 400, and 230 mJ, respectively. The repetition rate is 10 Hz, and the pulse duration is 5 ns. In the detection module, the USP LiDAR system has three elastic channels (355 nm, 532 nm, and 1064 nm) and three Raman channels (387 nm, 408 nm, and 530 nm). The system reaches full overlap at 300 m a.g.l. and operates with spatial and temporal resolutions of 7.5 m and 60 s, respectively (Lopes et al., 2019). The USP LiDAR station is part of the Latin America Lidar Network (http://lalinet.org), which is dedicated to measuring aerosol and particle distributions throughout Latin America (Guerrero-Rascado et al., 2016). The profiles of aerosol optical properties (i.e., backscatter and extinction profiles) were retrieved independently by applying Raman techniques (Ansmann and Müller, 2006). Thus, it is possible to directly measure the extinction-to-backscatter ratio (LiDAR ratio), which is a key parameter for aerosol characterization (Müller et al., 2007).
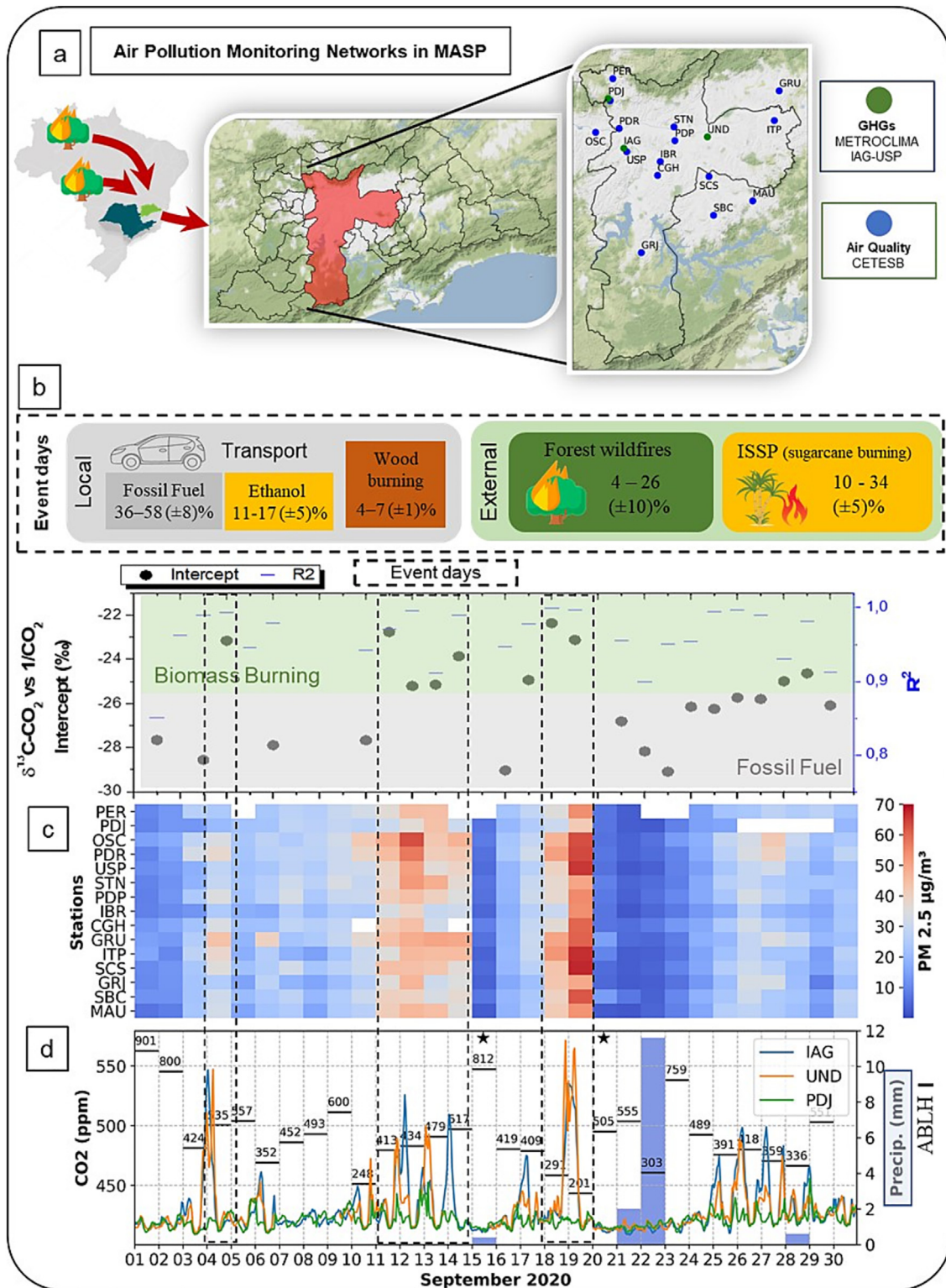
**Fig. 1.** Smoke plume detection in the Metropolitan Area of São Paulo (MASP). At air quality and greenhouse gas (GHG) monitoring networks (a), various techniques were employed to identify smoke plumes and quantify the impact of those events at the surface. Carbon isotopes measured in $CO_2$ (b) showed a predominance of biomass burning signatures on specific days (event days). Those signatures were confirmed by higher concentrations of fine particulate matter ($PM_{2.5}$, in c), $CO_2$ (in d), as well as other gases (CO and $CH_4$) and ratios ($CO/CO_2$ and $CH_4/CO_2$). In addition, back trajectories were used in order to confirm the provenance of the signatures. Certain meteorological conditions, such as atmospheric boundary layer height (ABLH, black lines), cold fronts (asterisk), and precipitation (blue bar), in combination with $CO_2$ concentrations, contributed to the accumulation of pollutants and cleaning of the atmosphere. On each event day, higher $PM_{2.5}$ and $CO_2$ concentrations were favored by a lower ABLH, especially on the most polluted day (September 19, 2020). On the days following each event day, cold fronts, precipitation, and higher ABLHs contributed to cleaning the atmosphere, as evidenced by the lower $PM_{2.5}$ and $CO_2$ concentrations. GHGs monitoring stations: USP, University of São Paulo; IAG, Institute of Astronomy, Geophysics, and Atmospheric Sciences; UND, UNICID - City University of São Paulo. CETESB, São Paulo State Environmental Protection Agency, Air quality stations: PER, Perus; PDJ, Pico do Jaraguá; OSC, Osasco; PDR, Ponte dos Remédios; STN, Santana; PDP, Parque Dom Pedro; IBR, Ibirapuera; CGH, Congonhas; GRU, Guarulhos; ITP, Itaim Paulista; SCS, São Caetano do Sul; GRJ, Grajaú; SBC, São Bernardo do Campo; MAU, Mauá.

### 2.6. Trajectory modeling

Air parcel back-trajectories were modeled with the National Oceanographic and Atmospheric Administration HYSPLIT, version 454. The modeling was performed by employing the Global Data Assimilation System (GDAS 1.0), a model space made available by the National Centers for Environmental Prediction, a branch of the National Weather Service. The HYSPLIT model was run with archived meteorological data to trace the transport of an air parcel vertically and horizontally through the atmosphere. To combine pollutant concentration data at the receptor site with back-trajectory data, the HYSPLIT model was run over a 120-h period. New back trajectories were simulated for air parcels arriving every 3 h at the MASP at a final elevation of 100 m a.g.l. We combined all trajectories simulated during each event observed in the MASP with pollutant concentration data provided by the CETESB and with the South American fires spot data provided by Brazilian National Institute for Space Research (INPE, 2020). The combined maps were made using the openair package and Igor Pro 7.0 (Wavemetrics, Portland, OR, USA). A PSCF was carried out in order to identify the potential source region for the air masses measured at the monitoring stations (Stein et al., 2015). The basis of PSCF is that if a source is located at, for example,

coordinates i and j, an air parcel back-trajectory passing through those coordinates indicates that material from the source can be collected and transported along the trajectory to the receptor site. The PSCF value can be interpreted as the conditional probability that concentrations larger than a given criterion value are related to the passage of air parcels through a grid cell with that PSCF value during transport to the receptor site. The criterion used here was the 90th percentile.

### 2.7. Classification of event and non-event days

In order to classify the days with abnormally higher contributions from wildfire- or generated smoke plumes to air pollution episodes, designated here as event days, we combined multiple approaches to distinguish signatures of external sources (forest wildfires and sugarcane burning) from local emissions (fossil and ethanol fuel combustion and wood burning, this last used at restaurants, pizza shops and bakeries) observed in the MASP during September 2020. Event days were selected on the basis of three criteria (Fig. S1): 1) higher concentrations of GHG, CO, and $PM_{2.5}$ at the majority (>95 %) of monitoring stations in the MASP; 2) Keeling plot intercepts ($\delta^{13}C\text{-}CO_2$ vs $1/CO_2$) most associated with C3 and C4 biomass burning



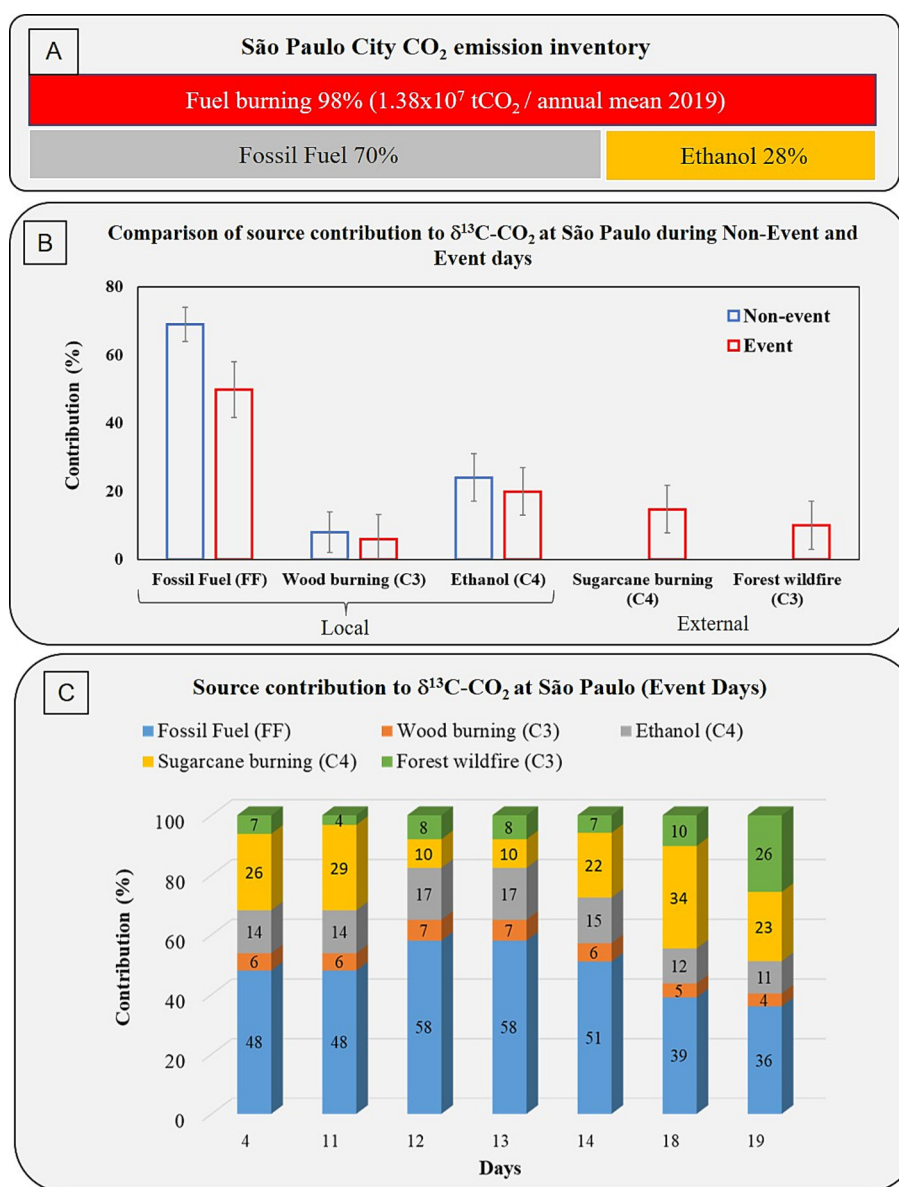**Fig. 2.** $CO_2$ source apportionment based on carbon isotopes and inventory data. A) Inventory data was based on fuel consumption at São Paulo city (www.gov.br/anp). B) $CO_2$ source apportionment based on $\delta^{13}C\text{-}CO_2$ and $CO/CO_2$ ratios mixing model (EPA-IsoSource).

signatures (Figs. 1b and S3); and 3) HYbrid Single Particle Lagrangian Integrated Trajectory (HYSPLIT) back trajectories related to wildfires from the northern region of the state (Figs. S5–11).

### 2.8. Fire weather and meteorological data

The Brazilian National Institute for Space Research is charged with monitoring fire activity throughout the country. Data related to the burned area, available since 2002, and fire spots, available since 1998, were obtained from the database of the Institute (INPE, 2020). Burned area data were estimated by an algorithm which relies on a burn-sensitive vegetation index, based on MODIS daily values of near and middle infrared reflectance, and makes use of active fire detection from multiple sensors (Libonati et al., 2015). Data and maps of climatological anomalies (temperature and precipitation, Figs. 4a and 5) were obtained from the Brazilian National Institute of Meteorology (INMET), which maintains a large database of meteorological and climatological parameters. Climatological normal are based on 438 meteorological surface stations measurements in continuous operations around Brazil. For each station temperature and precipitation normal are calculated by monthly averages (1981–2010). And anomalies are estimated by differences between monthly average, Sept-2020, against Brazilian climatological normal (Diniz et al., 2018).

### 3. Results

#### 3.1. Discrimination of event and non-event days

The differences between event and non-event days was assessed based on the levels of air pollutants ($PM_{2.5}$ and CO) and GHGs ($CO_2$ and $CH_4$) at various monitoring stations within the MASP (Fig. 1a). Remarkable increases in the GHG (Fig. S2A), CO (Fig. S2B), and $PM_{2.5}$ (Fig. 1c) concentrations were observed at >95 % of the monitoring stations during event days (September 4, 11, 12, 13, 14, 18, and 19). Days with concentration higher than 25 µg m$^{-3}$ (WHO standard), which exceeded the 24-h average on the 90 % of monitoring stations, were classified as $PM_{2.5}$ higher concentration days. Days with elevated GHG and CO were defined as those on which the peak concentrations were above the 3rd quartile (75th percentile) of the monthly average.

Evidences of higher pollutant concentrations in the MASP and smoke plume source, was supported by two findings: 1) $CO/CO_2$, $CH_4/CO_2$, and $CO/PM_{2.5}$ ratios and 2) stable $C-CO_2$ isotopes. In the first approach, noticeably higher $CO/CO_2$ and $CO/PM_{2.5}$ ratios were observed on event days in comparison to on non-event days (Fig. S4). For instance, the slope of CO vs $PM_{2.5}$ linear trend is 64 % higher for event days in relation to non-event (Fig. S4C). A number of other studies have detected these signatures of biomass burning (higher $PM_{2.5}$, GHG, and CO concentrations), as well as reporting higher $CO/CO_2$, $CH_4/CO_2$, and $CO/PM_{2.5}$ ratios modeled/measured in smoke plumes from wildfires (Amaral et al., 2019; Andreae et al., 2012; Laing et al., 2017; Squizzato et al., 2021; Zhao et al., 2021).

The second step was to compare $\delta^{13}C-CO_2$ values and $CO_2$ concentrations, known as the Keeling plot method (Pataki et al., 2003). Linear regression of daily data produced different intercept values, associated with the mixture of isotopic signatures of the main $CO_2$ sources, which predominated during event and non-event days (Fig. 1b). During non-event days, $CO_2$ emissions from fossil fuel ($\delta^{13}C-CO_2 \sim -32$ ‰, 69 %) and ethanol (C4, $\delta^{13}C-CO_2 \sim -12$ ‰, 21 %) predominated, as the main sources, in accordance with annual inventory and fuel consumption in the City (Fig. 2A). Local wood burning (C3, $\delta^{13}C-CO_2 \sim -25$ ‰, 8 %) mainly from pizza shops, which is known as an important pollutant source of particles and gases at MASP, currently is not accounted in the CO2 emission inventory (Andrade et al., 2017). Therefore, account contribution of local wood burning by $CO_2$ isotopic signatures is a good approach to distinguish the impact of external forest wildfires.

To differentiate, during event days, between local ethanol fuel combustion contribution (11–17 %) from external sugarcane burning (10–34 %) source (C4, $\delta^{13}C-CO_2 \sim -12$ ‰), both with similar $\delta^{13}C-CO_2$ values, the

ethanol vs fossil fuel ratio (Et/FF $\sim$ 0.35) was used. Similar Et/FF values were observed for $CO_2$ annual inventory and during non-event days, which comprises in a relevant approach to validate our $CO_2$ source apportionment estimation. In this line, the wood burning versus fossil fuel ratio (WB/FF $\sim$ 0.12), empirically obtained during non-event days, was employed to calculate local wood burning contributions (4–7 %) and distinguish from forest wildfires (4–26 %) during event days (Fig. 2B).

In the third step, we coupled $PM_{2.5}$, GHG, and CO concentrations with back trajectories to identify the main source associated with the higher concentrations observed on event days (Figs. S5–8). Back trajectories from the north/northwest predominated on event days (Fig. S9). Higher density of fire spot distribution, associated to forest wildfires and sugarcane burning and back trajectories from the north/northwest, confirmed the main sources of smoke plumes (Fig. S10). In addition, the Potential Source Contribution Function (PSCF) (Fleming et al., 2012; Pekney et al., 2006) was used to estimate the origin of high $PM_{2.5}$ concentrations on event days. The probability of higher $PM_{2.5}$ concentrations was found to be greatest from the north/northwest direction than south/southeast (Fig. S11), which was in accordance with back trajectories, corroborate that there were major contributions of smoke plumes from Amazonian and Pantanal wildfires and ISSP sugarcane burning.

#### 3.2. Smoke plume detection in the MASP

We combined multiple approaches to analyze smoke plume transport and the signatures of biomass burning observed in the MASP during September 2020. By monitoring the optical properties and vertical distribution of aerosols over the MASP with Raman LiDAR, we detected decoupling of the aerosol layer, above the ABL, on some event days (Fig. 3). Those aerosols were linked to the smoke plumes from wildfires in the Amazon and Pantanal forests and ISSP sugarcane burning as well, as shown by satellite images (Fig. 3a), HYSPLIT back trajectories, and LiDAR ratios (Fig. 3b). On September 13, the LiDAR station at the University of São Paulo detected an intense load of aerosol trapped within the ABL (at 3500 m of altitude) and several decoupled aerosol layers above the ABL (at 4000–5800 m). Two thin peaks at approximately 4200 m and 5000 m, respectively, presented LiDAR ratios of approximately 75 sr at 532 nm and 40 sr at 355 nm (Fig. 3b), typical of aerosols associated with biomass burning (Nicolae et al., 2013; Veselovskii et al., 2020). Similar decoupled plumes were observed on September 16 and 17 (Fig. S12) and mainly during the day on September 19, when the LiDAR system detected several prominent layers at 3000–5000 m (Fig. 3c).

To track transport of forest wildfires and sugarcane burning during event days, and associate with different contributions (Fig. 2), HYSPLIT modeling was combined with atmospheric boundary layer height (ABLH) and LiDAR observation. HYSPLIT back trajectories showed that particles which arrived at MASP in lower altitudes (250 m) during day 14, travel from the emission source into ABL (Fig. S13A), suggesting major contributions from nearby sources as sugarcane burning at ISSP (22 %) than forest wildfires (10 %). Similar results are true to days 04 and 11 (Fig. S14A), in accordance with $CO_2$ source apportionment estimation based on carbon isotopes. During day 19, which presented higher pollution episode and major contribution of forest wildfires (26 %), HYSPLIT back trajectories (Fig. S13) presented particles originated during day 17 from distant forested area source travelling above ABL followed by intrusion during day 18, in agreement with prominent layers detected by LiDAR and surface measurements (Fig. 3). However, understanding the role that meteorological conditions played in the intrusion of plumes and the accumulation of pollutants on the event days, especially during day 19, is necessary to perform a comprehensive analysis of the sources, transport, and mechanisms of air pollution in the MASP caused by external wildfire events.

#### 3.3. Meteorological conditions promoting event days and the impact on air quality and $CO_2$ excess

When variations in the concentrations of GHG, $PM_{2.5}$, and CO were assessed against meteorological parameters, ABLH, atmospheric stability,
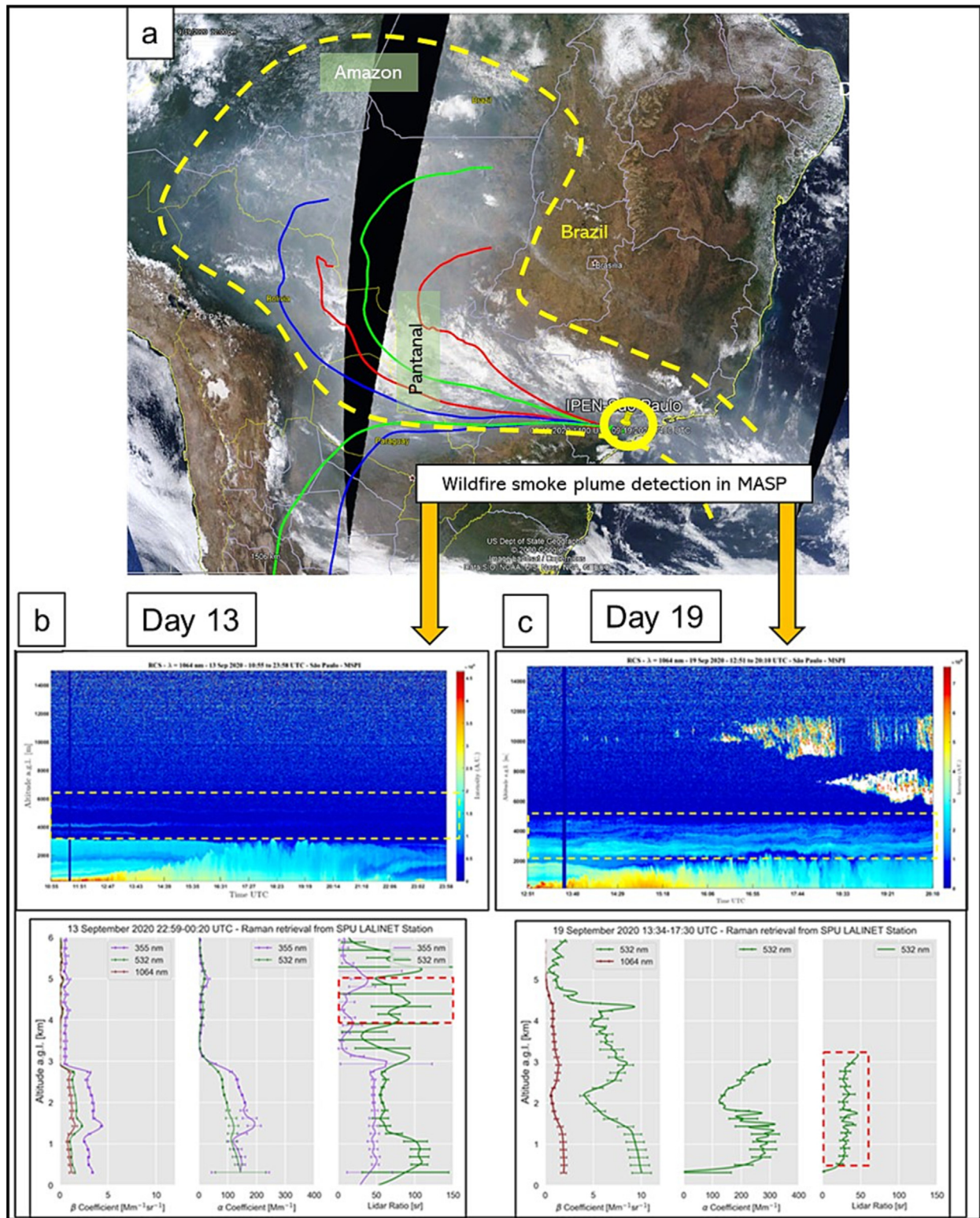
**Fig. 3.** Transport of smoke plumes from Pantanal wildfires and detection of those aerosol layers in the Metropolitan Area of São Paulo (MASP) by remote sensing. a) Satellite images show smoke plumes transported from the Pantanal to the MASP, back trajectories calculated by the HYbrid Single Particle Lagrangian Integrated Trajectory model confirming the origin and transport of the plumes. The optical properties and vertical distribution of the aerosol layers were monitored by the Raman LiDAR system. b) Decoupled aerosol layers (yellow dotted lines), observed between 4800 m and 5000 m of altitude, above the atmospheric boundary layer, presented LiDAR ratios linked to biomass burning signatures (red dotted lines). c) On the most polluted day (September 19, 2020), the LiDAR system detected several prominent aerosol layers at altitudes of 3000–5000 m (yellow dotted lines). USP, University of São Paulo; LALINET, Latin America Lidar Network.

and wind direction were found to be important determinants of event days (Fig. 4b). Negative correlations were observed between pollutant concentrations and ABL height (Fig. S15). On the event days, September 4, 11,

12, 13, 14, and 18, ABL instability clearly contributed to the intrusion of smoke plumes into the mixed layer (Fig. S16A) particularly during day 18, in accordance with HYSPLIT modeling previously discussed. On the
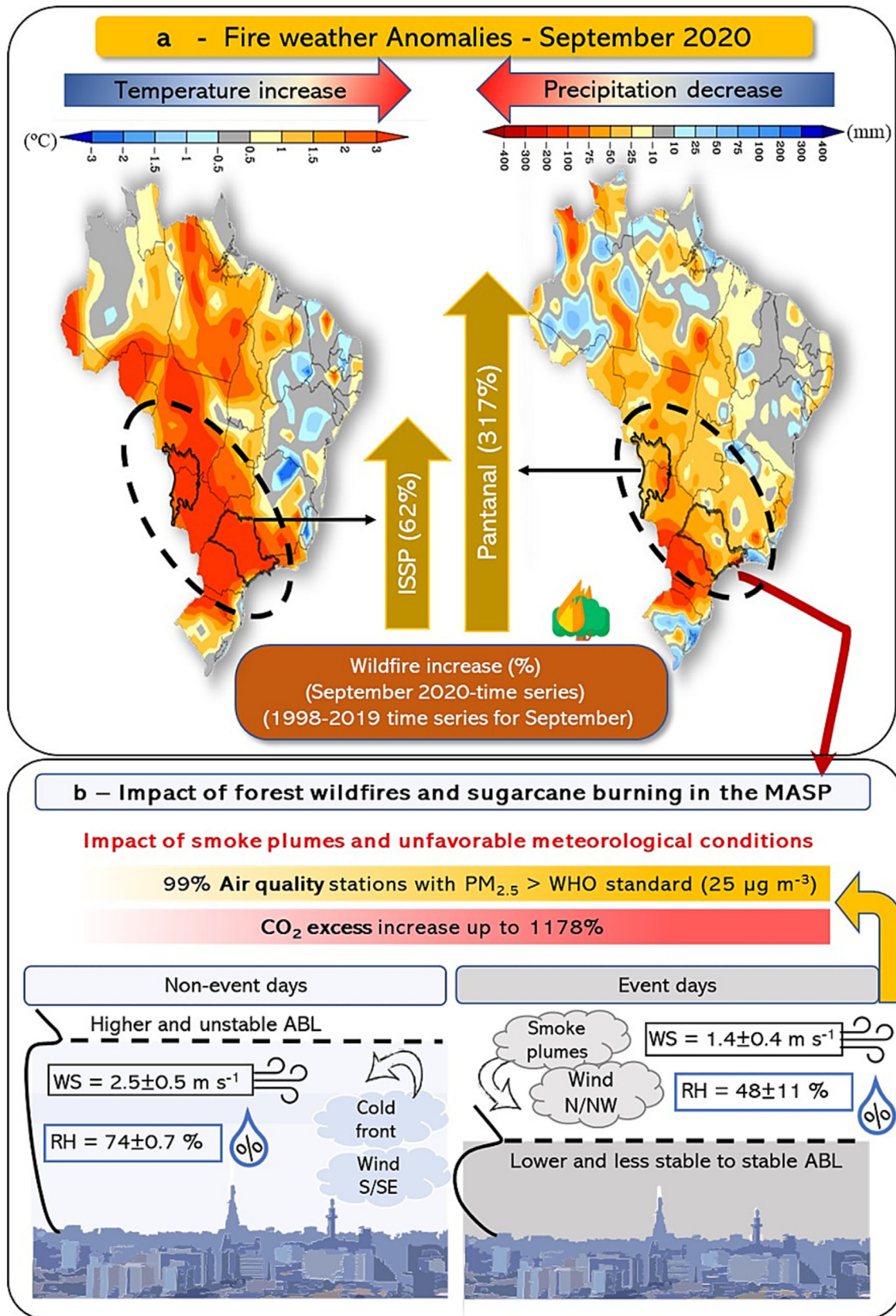
**Fig. 4.** Distribution of fire weather anomalies in Brazil and increases in the number of fires during September 2020, in relation to the 1998–2019 time series average, in the Pantanal and interior of the state of São Paulo (ISSP). a) In both regions, there were record numbers of fires in September 2020. b) Smoke plumes from the wildfires in the Pantanal and ISSP reached the Metropolitan Area of São Paulo (MASP) and combined with unfavorable meteorological conditions to promote days on which there were high concentrations of pollutants (event days). On the event days, marked impacts on air quality were observed as exceedances of the World Health Organization (WHO) standard (of 25 μg m$^{-3}$) for 24-h concentrations of fine particulate matter (PM$_{2.5}$) at 99 % of the air quality monitoring stations and 100–1178 % higher hourly average CO$_2$ excess. ABL, atmospheric boundary layer; WS, wind speed; RH, relative humidity.

most polluted day (September 19), a highly stable ABL favored pollutant accumulation (Fig. S16B). In addition, the northerly/northwesterly wind direction in the layers above the ABL confirmed that, on event days, the smoke plumes originated from the forest wildfires and ISSP sugarcane burning regions, in alignment with LiDAR remote sensing and HYSPLIT modeling (Figs. 3 and S5–14). On the days following the event days (September 15, 20, 21, 22, and 23), pollutant dispersion was favored by cold fronts moving inland from the coast (south/southeast) and rainfall (Figs. 1d and S5–8), together with higher ABLs and unstable conditions (Fig. S17). Aligned with those conditions, non-event days were characterized by higher average wind speed ($2.2 \pm 0.4$ m s$^{-1}$), higher average relative humidity ($68 \pm 11$ %) and lower average temperature ($20 \pm 3$ °C), in opposite with event days meteorology conditions (Figs. 4b and S18).

Smoke plume intrusion had a marked impact on air quality and $CO_2$ concentration. (Fig. S19A). In addition, more than half of the days on which PM2.5 concentrations exceeded the WHO standard ($>25$ μg m$^{-3}$) in September 2020 were attributed to event days (Fig. S19B). Diurnal cycle variations in $CO_2$ concentrations were calculated by comparing the hourly average $CO_2$ concentrations measured at two urban monitoring stations (IAG and UND) with those measured at a background monitoring station (PDJ) (Fig. S20A). The $CO_2$ variability over the day is result of ABL dynamic, photosynthesis and sources. On the midday and early afternoon $CO_2$ decrease is due higher ABL heights and photosynthetic activity, whereas, during nighttime higher $CO_2$ concentrations are associated with lower ABL heights and accumulation of $CO_2$. As expected, $CO_2$ concentrations at the urban monitoring stations were higher on event days than on non-event days, the difference ranging from 10 ppm to 70 ppm during nighttime (19 h to 06 h) and early morning (06 h to 08 h), whereas no appreciable differences between event and non-event days were observed at the background monitoring station (Fig. S20A). The $CO_2$ excess was estimated by hourly mean $CO_2$ concentrations at IAG and UND stations against background station (PDJ). Therefore, $CO_2$ excess are related to the $CO_2$ concentration above the $CO_2$ urban background concentrations. During non-event days $CO_2$ excess at IAG and UND stations were lower than 20 ppm, whereas during event days the values were higher than 50 ppm with peak above 80 ppm at UND (Fig. S20B). Differences of $CO_2$ excess between non-event and event days ranged from 100 to 1178 %, which account to the level of importance of those external sources, associated with biomass burning events of forest and sugarcane harvest, to increase of $CO_2$ levels in the metropolitan areas as RMSP.

### 3.4. Potential sources of ignition of the forest wildfires and interior of the state of São Paulo (ISSP)

Considering the relevance of external biomass burning events to vulnerability of air quality at MASP, assessment of the main causes of current extreme wildfires is relevant to help in the mitigation policies. Recent studies have demonstrated that fire weather, in combination with natural seasonality and climate change forcing mechanisms, intensifies wildfires in various forests worldwide (Goss et al., 2020; Abram et al., 2021). In September 2020 in the Pantanal and ISSP, humidity and precipitation totals were lower than normal, whereas temperature anomalies and wildfires were more frequent than normal (Fig. 4a). To investigate the role of fire weather, linked to temperature/precipitation anomalies and relative humidity, with the recent occurrence of extreme wildfires in these areas, we examined trends in the relationships between fire weather and wildfire data (number of fires and area burned) between 2010 and 2020 (Figs. 5 and S21). We found moderate to significant correlations between fire weather variables and wildfire data over the 2010–2019 in the Pantanal ($r = 0.40$–$0.69$, $p < 0.01$ for all). However, the number of fire spots detected during September 2020 (8106) was 181 % higher than the 2887 fire spots detected in September 2019 and 317 % higher than the monthly time series average of 1944 fire spots during the 1998–2019 period (Fig. 4a). The area burned increased by 120 % and 207 %, respectively, in comparison with the previous year and the time series average for the 2002–2019 period (14,264 km$^2$ vs. 6476 km$^2$ and 4646 km$^2$, respectively). The number of fires and the area
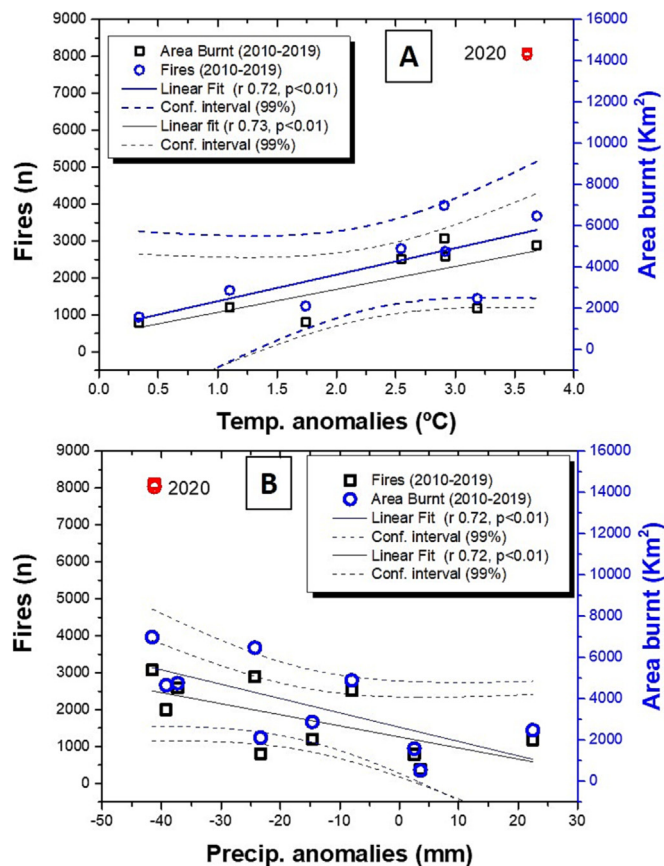


**Fig. 5.** Fire weather trends. The fire weather trends were analyzed by identifying correlations between wildfire parameters (number of fires and area burned) and weather anomalies (A - temperature and B - precipitation) in the Pantanal, by using time series (2010–2020) averages for the month of September. All data were provided by Brazilian National Institute for Space Research (INPE) and Brazilian National Institute of Meteorology (INMET). The extreme wildfires occurring in 2020 in the Pantanal (red points) are characterized as outlier event in relation to the fire weather trends over the preceding 10 years.

burned in the Pantanal both set all-time records during September 2020. Those extremes are clearly outliers from the fire weather trends observed in the Pantanal (Fig. 5), suggesting that wildfire events are attributable to causes other than just the weather.

One major regional source of smoke plumes transported to the MASP is biomass burning related to agricultural activity. The western and northern regions of the ISSP are dedicated to agriculture, especially sugarcane cultivation, which involves the burning of agricultural residues (Held et al., 2012). During the 2010–2020 period in the Pantanal and ISSP (Fig. S21), there were moderate-to-strong correlations between the number of fire spots and the occurrence of temperature/precipitation anomalies ($r = 0.70$–$0.89$, $p < 0.01$), whereas there was a very strong correlation between the number of fires spots and the relative humidity ($r = 0.94$, $p < 0.01$). The number of fire spots in the ISSP was 101 % and 62 % higher in September 2020 than in September 2019 and in the 1998–2019 times series for September, respectively. Despite that increase, fire spot numbers in the ISSP remained aligned with the fire weather trends, even when extreme weather events are taken into account, in contrast to what was found for the Pantanal wildfires of 2020, which supports our hypothesis of an abnormal event in the Pantanal.

### 4. Discussion and conclusion

Our study presents the first comprehensive analysis to clarify how smoke plumes originating mainly from Amazonian and Pantanal wildfires combined with sugarcane burning from ISSP arrived in the MASP, where

they worsened air quality, resulting in PM2.5 concentration exceeding WHO standards ($>25$ $\mu$g m$^{-3}$) and elevated GHGs concentrations. Our analysis involved different approaches, including trajectory modeling, remote sensing, surface measurements monitoring of air quality (PM$_{2.5}$ and CO) and GHGs, as well as the CO$_2$ source apportionment based on carbon isotopic signatures and the evaluation of atmospheric dynamics. Smoke plumes were identified by LiDAR ratio at high altitudes over the MASP. The presence of those plumes at the surface were confirmed by detecting various markers, such as peak concentrations of PM$_{2.5}$, GHG, and CO, and determining the specific ratios between species (CO/CO$_2$, CH$_4$/CO$_2$ and PM$_{2.5}$/CO), as well as quantified by mix modeling, using $\delta^{13}$C-CO$_2$ values and CO/CO$_2$ ratio, associated with forest (4–26 %) and sugarcane (10–34 %) biomass burning and local urban sources (51–82 %) during event days. Intrusion of smoke plumes into the urban atmosphere was favored by unstable conditions in the ABL, followed by accumulation of pollutants resulting in the most polluted day 19, with higher contributions of forest (26 %) and sugarcane (23 %) smoke plumes, when lower ABL height predominated and there was atmospheric stability.

We also provided valuable information about the risks that external sources such as wildfires and agricultural burning pose to large urban areas, due worsening air quality and altering the GHG budget in densely occupied regions, which is a worldwide threat. To our knowledge, this is the first study quantifying the impact that the smoke plumes from the forest wildfires combined with sugarcane burning at ISSP in September 2020 had on the MASP. On event days, 99 % of air quality monitoring stations recorded PM$_{2.5}$ concentrations above the WHO standard, those concentrations being responsible for $>50$ % of the exceedances of WHO standards during September. In addition, hourly average CO$_2$ excesses were 100–1178 % higher on event days than on non-event days. In accordance with our findings, previous studies have reported the impact that the transport of pollutants from wildfires have had on air quality in various cities in the United States (Liu et al., 2017; Rogers et al., 2020).

Wildfires pose an extra challenge for cities committed to achieving the Paris Agreement goals, given that urban activities are responsible for $>60$ % of GHG emissions (UN, n.d.-a). Therefore, the role of external sources of GHG, such as wildfires, must be assessed in order to address potential enhancement that the warming effects have on the GHG budget in densely populated urban areas (Revi et al., 2014). Therefore, it is imperative to perform continuous monitoring of GHG concentrations and employ source tracing strategies, such as the identification of isotopic signatures, in order to assess local sources of GHGs, determine atmospheric GHG levels over time, validate emission inventories, and understand external inputs (Duren and Miller, 2020). For instance, if the CH$_4$ increase observed over the past decade, the causes of which have yet to be defined, continues at the current rate ($>5$ ppb/year), the consequent climate warming impact will make it impossible to meet the goals of the Paris Agreement (Nisbet et al., 2019).

In this line causes of extreme events must be investigated in order to implement policies to mitigation strategies. Our analysis showed that, for the month of September in the Pantanal, the area burned increased by 207 % and fire spots increased by 317 % between 2020 and time series average (1998–2019). Therefore, the extreme event of September 2020 must be further assessed as an outlier in relation to fire weather trends observed in the Pantanal time series. These results underscore the need for further investigation to identify the causes of those extreme wildfires. The last Brazilian government measures to reduce environmental protections, such as weakening environmental agencies, changing the forest code to grant amnesty to those who engage in illegal deforestation, reducing the size of protected areas, cutting resources for conservation, and passing lax legislation, have been cited as the main risks to forest safety and may have contributed to the unprecedented fires in the Pantanal in 2020 (Ferrante and Fearnside, 2019; Libonati et al., 2020). Unfortunately, given the projected fire emissions in all Brazilian biomes-the Pantanal, Amazon, savanna (Cerrado), shrublands (Caatinga), Atlantic Forest, and pampas—the continuation of the current environmental policies will result in annual CO$_2$ emissions exceeding 5.7 Gt in 2030. That will impair the ability of Brazil to meet the target of a 43 % reduction in GHG emissions by 2030 (in relation to 2015 levels), as pledged in the Paris Agreement (da Silva Junior et al., 2020). In addition to local environmental threats, fire weather conditions (e.g. temperature, precipitation, and drought), intensified by climate change, have contributed to increasing the likelihood of fire activity, including extreme wildfires, worldwide, as recently reported in Australia and California (Abatzoglou et al., 2019; Goss et al., 2020; IPCC, 2018; Marengo et al., 2021; Nisbet et al., 2019).

## CRediT authorship contribution statement

CES-O GHG measurements, data acquisition and processing, manuscript write, figures and analysis. M.T.A.M GHG measurements, data acquisition and processing, figures, analysis and manuscript review. T.N. manuscript write and review, Hysplit and PSCF figures and analysis. F.J.S.L. Lidar analysis, figures and interpretation/methodology write. J.A.G.M. GHG measurements. I.M.M.A.M. GHG measurements. G.A.M. ABLH analysis. P.L.S.D. manuscript review, E.L. funds acquisition and manuscript review. M.F.A. funds acquisition, manuscript write and review.

## Data availability

Data will be made available on request.

## Declaration of competing interest

Carlos Souto-Oliveira reports financial support was provided by State of Sao Paulo Research Foundation (FAPESP).

## Appendix A. Supplementary data

Supplementary data to this article can be found online at https://doi.org/10.1016/j.scitotenv.2023.163439.

## References

Abatzoglou, J.T., Williams, A.P., Barbero, R., 2019. Global emergence of anthropogenic climate change in fire weather indices. Geophys. Res. Lett. 46 (1), 326–336. https://doi.org/10.1029/2018GL080959.

Abram, N.J., Henley, B.J., Sen Gupta, A., Lippmann, T.J.R., Clarke, H., Dowdy, A.J., Sharples, J.J., Nolan, R.H., Zhang, T., Wooster, M.J., Wurtzel, J.B., Meissner, K.J., Pitman, A.J., Ukkola, A.M., Murphy, B.P., Tapper, N.J., Boer, M.M., 2021. Connections of climate change and variability to large and extreme forest fires in southeast Australia. Commun. Earth Environ. 2, 1–17. https://doi.org/10.1038/s43247-020-00065-8.

Amaral, S.S., Costa, M.A.M., Soares Neto, T.G., Costa, M.P., Dias, F.F., Anselmo, E., Santos, J.C. dos, Carvalho, J.A. de, 2019. CO$_2$, CO, hydrocarbon gases and PM2.5 emissions on dry season by deforestation fires in the Brazilian Amazonia. Environ. Pollut. 249 (March), 311–320. https://doi.org/10.1016/j.envpol.2019.03.023.

Andrade, M.F., Ynoue, R., Martins, L.D., 2017. Air quality in the megacity of São Paulo: evolution over the last 30 years and future perspectives. Atmos. Environ. 159 (October), 66–82. https://doi.org/10.1016/j.atmosenv.2017.03.051.

Andreae, M.O., Artaxo, P., Beck, V., Bela, M., Freitas, S., Gerbig, C., Longo, K., Munger, J.W., Wiedemann, K.T., Wofsy, S.C., 2012. Carbon monoxide and related trace gases and aerosols over the Amazon Basin during the wet and dry seasons. Atmos. Chem. Phys. 12 (13), 6041–6065. https://doi.org/10.5194/acp-12-6041-2012.

Ansmann, A., Müller, D., 2006. Lidar and atmospheric aerosol particles. Lidar. Springer, 2006, pp. 105–141. https://doi.org/10.1007/0-387-25101-4_4.

Balch, J.K., Bradley, B.A., Abatzoglou, J.T., Chelsea Nagy, R., Fusco, E.J., Mahood, A.L., 2017. Human-started wildfires expand the fire niche across the United States. PNAS 114 (11), 2946–2951. https://doi.org/10.1073/pnas.1617394114.

da Silva Junior, C.A., Teodoro, P.E., Delgado, R.C., Teodoro, L.P.R., Lima, M., de Andréa Pantaleão, A., Baio, F.H.R., de Azevedo, G.B., de Oliveira Sousa Azevedo, G.T., Capristo-Silva, G.F., Arvor, D., Facco, C.U., 2020. Persistent fire foci in all biomes

undermine the Paris Agreement in Brazil. Sci. Rep. 10 (1), 1–14. https://doi.org/10.1038/s41598-020-72571-w.

Diniz, F.A., Ramos, A.M., Rebello, E.R.G., 2018. Brazilian climate normals for 1981–2010. Pesqui. Agropecu. Bras. 53, 131–143.

Duren, R.M., Miller, C.E., 2020. Measuring the carbon emissions of megacities. Nat. Publ. Group 2 (August 2012). https://doi.org/10.1038/nclimate1629.

Escobar, H., 2019. Amazon fires clearly linked to deforestation, scientists say. Science 365 (6456), 853. https://doi.org/10.1126/science.365.6456.853.

Ferrante, L., Fearnside, P.M., 2019. Brazil's new president and "ruralists" threaten Amazonia's environment, traditional peoples and the global climate. Environ. Conserv. 10–12. https://doi.org/10.1017/S0376892919000213.

Fleming, Z.L., Monks, P.S., Manning, A.J., 2012. Review: untangling the influence of air-mass history in interpreting observed atmospheric composition. Atmos. Res. 104–105, 1–39. https://doi.org/10.1016/j.atmosres.2011.09.009.

Gonino, G.M.R., Figueiredo, B.R.S., Manetta, G.I., Zaia Alves, G.H., Benedito, E., 2019. Fire increases the productivity of sugarcane, but it also generates ashes that negatively affect native fish species in aquatic systems. Sci. Total Environ. 664, 215–221. https://doi.org/10.1016/j.scitotenv.2019.02.022.

Goss, M., Swain, D.L., Abatzoglou, J.T., Sarhadi, A., Kolden, C.A., Williams, A.P., #38; Diffenbaugh, N. S., 2020. Climate change is increasing the likelihood of extreme autumn wildfire conditions across California. Environ. Res. Lett. 15 (9). https://doi.org/10.1088/1748-9326/ab83a7.

Guerrero-Rascado, J.L., Landulfo, E., Antuña, J.C., de Melo Jorge Barbosa, H., Barja, B., Bastidas, Á.E., Bedoya, A.E., da Costa, R.F., Estevan, R., Forno, R., Gouveia, D.A., Jiménez, C., Larroza, E.G., da Silva Lopes, F.J., Montilla-Rosero, E., de Arruda Moreira, G., Nakaema, W.M., Nisperuza, D., Alegria, D., Silva, A., 2016. Latin American Lidar Network (LALINET) for aerosol research: diagnosis on network instrumentation. J. Atmos. Sol. Terr. Phys. 138–139, 112–120. https://doi.org/10.1016/j.jastp.2016.01.001.

Held, G., Allen, G.A., Lopes, F.J.S., Gomes, A.M., Cardoso, A.A., Landulfo, E., 2012. Review of aerosol observations by Lidar and chemical analysis in the state of São Paulo, Brazil. Atmospheric Aerosols - Regional Characteristics - Chemistry and Physics (InTech, 2012) https://doi.org/10.5772/50737.

INPE, Instituto Nacional de Pesquisas Espaciais, 2020. Portal de Monitoramento de Queimadas e Incêndios Florestais.Available at. http://www.inpe.br/queimadas (Accessed 14 december 2020).

IPAM-Amazônia, 2020. About 17.5% of Brazil has burned at least once in the last 20 years. Available at https://ipam.org.br/17-5-of-brazil-has-burned-at-least-once-in-the-last-20-years Accessed 24 march 2021.

IPCC, 2018. Expert Meeting on Short-Lived Climate Forcers (SLCF) Meeting Report.28–31 May. Geneva, Switzerland. Available at: https://www.ipcc-nggip.iges.or.jp/public/mtdocs/pdfiles/1805_Expert_Meeting_on_SLCF_Report.pdf (Accessed 18 january 2022).

Ivory, S.J., McGlue, M.M., Spera, S., Silva, A., Bergier, I., 2019. Vegetation, rainfall, and pulsing hydrology in the Pantanal, the world's largest tropical wetland. Environ. Res. Lett. 14 (12). https://doi.org/10.1088/1748-9326/ab4ffe.

Jolly, W.M., Cochrane, M.A., Freeborn, P.H., Holden, Z.A., Brown, T.J., Williamson, G.J., Bowman, D.M.J.S., 2015. Climate-induced variations in global wildfire danger from 1979 to 2013. Nat. Commun. 6 (May), 1–11. https://doi.org/10.1038/ncomms8537.

Jones, M.W., Smith, A.J.P., Betts, R., Canadell, J.G., Prentice, I.C., Le Quéré, C., 2020. Climate change increases the risk of wildfires. Sci. Brief Rev.

Laing, J.R., Jaffe, D.A., Slavens, A.P., Li, W., Wang, W., 2017. Can ΔPM2.5/ΔCO and ΔNOy/ΔCO enhancement ratios be used to characterize the influence of wildfire smoke in urban areas? Aerosol Air Qual. Res. 17 (10), 2413–2423. https://doi.org/10.4209/aaqr.2017.02.0069.

Libonati, R., DaCamara, C.C., Setzer, A.W., Morelli, F., Melchiori, A.E., 2015. Na algorithm for burned area detection in the Brazilian Cerrado using 4 μm MODIS imagery. Remote Sens. 7, 15782–15803. https://doi.org/10.3390/rs71115782.

Libonati, R., Dacamara, C.C., Peres, L.F., Carvalho, L.A.S. de, Garcia, L.C., 2020. Rescue Brazil's Burning Pantanal Wetlands.

Liu, X., Huey, L.G., Yokelson, R.J., Selimovic, V., Simpson, I.J., Müller, M., Jimenez, J.L., Campuzano-Jost, P., Beyersdorf, A.J., Blake, D.R., Butterfield, Z., Choi, Y., Crounse, J.D., Day, D.A., Diskin, G.S., Dubey, M.K., Fortner, E., Hanisco, T.F., Hu, W., Wolfe, G.M., 2017. Airborne measurements of western U.S. wildfire emissions: comparison with prescribed burning and air quality implications. J. Geophy. Res. 122 (11), 6108–6129. https://doi.org/10.1002/2016JD026315.

Lopes, F.J.S., Silva, J.J., Marrero, J.C.A., Taha, G., Landulfo, E., 2019. Synergetic aerosol layer observation after the 2015 Calbuco volcanic eruption event. Remote Sens. 11, 195.

Marengo, J.A., Cunha, A.P., Cuartas, L.A., Leal, K.R.D., Broedel, E., Seluchi, M.E., Michelin, C.M., Flávia, C., Baião, D.P., Ângulo, E.C., Almeida, E.K., 2021. Extreme Drought in the Brazilian Pantanal in 2019–2020: Characterization, Causes, and Impacts. 3. https://doi.org/10.3389/frwa.2021.639204 (February).

Mega, E.R., 2020. 'Apocalyptic' fires are ravaging the world's largest tropical wetland. Nature 586, 20–21.

Müller, D., et al., 2007. Aerosol-type-dependent lidar ratios observed with Raman lidar. J. Geophys. Res. Atmos. 112, 16202.

NASA Earth Observatory, 2020. Fires Char the Pantanal.Available at: https://earthobservatory.nasUntitledFoldera.gov/images/147269/fires-char-the-pantanal (Accessed 05 october 2020).

Neves, L.A., Rodrigues, J.M., Daroda, R.J., Silva, P.R.M., Ferreira, A.A., Aranda, D.A.G., Eberlin, M.N., Fasciotti, M., 2015. The influence of different referencing methods on the accuracy of δ13C value measurement of ethanol fuel by gas chromatography/combustion/isotope ratio mass spectrometry. Rapid Commun. Mass Spectrom. 29 (21), 1938–1946. https://doi.org/10.1002/rcm.7298.

Nicolae, D., Nemuc, D., Müller, C., Talianu, J., Vasilescu, L., Belegante, A. Kolgotin, 2013. Characterization of fresh and aged biomass burning events using multiwavelength Raman lidar and mass spectrometry. J. Geophys. Res. Atmos. 118, 2956–2965 (2013).

Nisbet, E.G., Manning, M.R., Dlugokencky, E.J., Fisher, R.E., Lowry, D., Michel, S.E., Myhre, C.L., Platt, S.M., Allen, G., Bousquet, P., Brownlow, R., Cain, M., France, J.L., Hermansen, O., Hossaini, R., Jones, A.E., Levin, I., Manning, A.C., Myhre, G., White, J.W.C., 2019. Very strong atmospheric methane growth in the 4 years 2014–2017: implications for the Paris Agreement. Glob. Biogeochem. Cycles 33 (3), 318–342. https://doi.org/10.1029/2018GB006009.

Pataki, D.E., Ehleringer, J.R., Flanagan, L.B., Yakir, D., Bowling, D.R., Still, C.J., Buchmann, N., Kaplan, J.O., Berry, J.A., 2003. The application and interpretation of keeling plots in terrestrial carbon cycle research. Glob. Biogeochem. Cycles 17 (1). https://doi.org/10.1029/2001GB001850.

Pekney, N., Davidson, C., Zhou, L., Hopke, P., 2006. Application of PSCF and CPF to PMF-modeled sources of PM2.5 in Pittsburgh. Aerosol Sci. Technol. 40, 952–961 (Taylor & Francis Group, 2006).

Perkins-Kirkpatrick, S.E., Lewis, S.C., 2020. Increasing trends in regional heatwaves. Nat. Commun. 11, 1–8.

Pinto, O.B., Marques, A.C.A., Vourlitis, G.L., 2020. Aboveground carbon storage and cycling of flooded and upland forests of the Brazilian Pantanal. Forests 11 (6), 1–15. https://doi.org/10.3390/f11060665.

Pivello, V.R., Vieira, I., Christianini, A.V., Ribeiro, D.B., da Silva Menezes, L., Berlinck, C.N., Melo, F.P.L., Marengo, J.A., Tornquist, C.G., Tomas, W.M., Overbeck, G.E., 2021. Understanding Brazil's catastrophic fires: causes, consequences and policy needed to prevent future tragedies. Perspect. Ecol. Conserv. 19 (3), 233–255. https://doi.org/10.1016/j.pecon.2021.06.005.

Reddington, C.L., Butt, E.W., Ridley, D.A., Artaxo, P., Morgan, W.T., Coe, H., Spracklen, D., v., 2015. Air quality and human health improvements from reductions in deforestation-related fire in Brazil. Nat. Geosci. 8 (10), 768–771. https://doi.org/10.1038/ngeo2535.

Revi, A., Satterthwaite, D.E., Aragón-Durand, F., Corfee-Morlot, J., Kiunsi, R.B.R., Pelling, M., Roberts, D.C., Solecki, W., 2014. Urban areas. In: Field, C.B., Barros, V.R., Dokken, D.J., Mach, K.J., Mastrandrea, M.D., Bilir, T.E., Chatterjee, M., Ebi, K.L., Estrada, Y.O., Genova, R.C., Girma, B., Kissel, E.S., Levy, A.N., MacCracken, S., Mastrandrea, P.R., White, L.L. (Eds.), Climate Change 2014: Impacts, Adaptation, and Vulnerability. Part A: Global and Sectoral Aspects. Contribution of Working Group II to the Fifth Assessment Report of the Intergovernmental Panel on Climate Change. Cambridge University Press, Cambridge, United Kingdom and New York, NY, USA , pp. 535–612. https://www.ipcc.ch/site/assets/uploads/2018/02/WGIIAR5-Chap8_FINAL.pdf.

Rogers, H.M., Ditto, J.C., Gentner, D.R., 2020. Evidence for impacts on surface-level air quality in the northeastern US from long-distance transport of smoke from North American fires during the Long Island Sound Tropospheric Ozone Study (LISTOS) 2018. Atmos. Chem. Phys. 20 (2), 671–682. https://doi.org/10.5194/acp-20-671-2020.

Satar, E., Berhanu, T.A., Brunner, D., Henne, S., Leuenberger, M., 2016. Continuous CO2/CH4/CO Measurements (2012–2014) at Beromünster Tall Tower Station in Switzerland. , pp. 2623–2635 https://doi.org/10.5194/bg-13-2623-2016.

Schumacher, M., Werner, R.A., Meijer, H.A.J., Jansen, H.G., Brand, W.A., Geilmann, H., Neubert, R.E.M., 2011. Oxygen isotopic signature of CO2 from combustion processes. Atmos. Chem. Phys. 11 (4), 1473–1490. https://doi.org/10.5194/acp-11-1473-2011.

Semmens, C., Ketler, R., Schwendenmann, L., Nesic, Z., Christen, A., 2014. Isotopic Composition of CO2 in Gasoline, Diesel and Natural Gas Combustion Exhaust in Vancouver, BC, Canada. September, 12 https://doi.org/10.13140/2.1.3929.0248.

Squizzato, R., Nogueira, T., Martins, L.D., 2021. Beyond megacities: tracking air pollution from urban areas and biomass burning in Brazil. npj Clim. Atmos. Sci., 1–7 https://doi.org/10.1038/s41612-021-00173-y.

Stein, A.F., Draxler, R.R., Rolph, G.D., Stunder, B.J.B., Cohen, M.D., Ngan, F., 2015. Noaa's hysplit atmospheric transport and dispersion modeling system. Bull. Am. Meteorol. Soc. 96 (12), 2059–2077. https://doi.org/10.1175/BAMS-D-14-00110.1.

Tomas, W.M., de Oliveira Roque, F., Morato, R.G., Medici, P.E., Chiaravalloti, R.M., Tortato, F.R., Penha, J.M.F., Izzo, T.J., Garcia, L.C., Lourival, R.F.F., Girard, P., Albuquerque, N.R., Almeida-Gomes, M., Andrade, M.H. da S., Araujo, F.A.S., Araujo, A.C., Arruda, E.C. de, Assunção, V.A., Battirola, L.D., Junk, W.J., 2019. Sustainability Agenda for the Pantanal Wetland: Perspectives on a Collaborative Interface for Science, Policy, and Decision-Making. In Tropical Conservation Science. vol. 12. https://doi.org/10.1177/1940082919872634 Issue September.

UN. United Nations, d. Climate Action: Cities and Pollution.Available at. https://www.un.org/en/climatechange/climate-solutions/cities-pollution (Accessed 23 april 2021).

UN. United Nations, 2018. The World's Cities in 2018. The World's Cities in 2018 - Data Booklet. Available at. https://www.un.org/en/events/citiesday/assets/pdf/the_worlds_cities_in_2018_data_booklet.pdf (Accessed 23 april 2021).

Veselovskii, I., et al., 2020. Variability in lidar-derived particle properties over West Africa due to changes in absorption: towards an understanding. Atmos. Chem. Phys. 20, 6563–6581.

WWF, 2020. Fires, Forests and the Future: A Crisis Ranging out of Control.Available at https://wwfeu.awsassets.panda.org/downloads/wwf_fires_forests_and_the_future_report.pdf (Accessed 17 january 2021).

Zhao, H., Yang, G., Tong, D.Q., Zhang, X., Xiu, A., Zhang, S., 2021. Interannual and Seasonal Variability of Greenhouse Gases and Aerosol Emissions from Biomass Burning in Northeastern China Constrained by Satellite Observations.